Deformation behavior and plastic instabilities of ultrafine-grained titanium

D. Jia, Y. M. Wang, K. T. Ramesh, and E. Ma[a)]
Departments of Mechanical Engineering and Materials Science and Engineering, The Johns Hopkins University, Baltimore, Maryland 21218

Y. T. Zhu
Division of Materials Science and Technology, Los Alamos National Laboratory, Los Alamos, New Mexico 87545

R. Z. Valiev
Institute of Physics of Advanced Materials, Ufa State Aviation Technical University, Ufa, 450000, Russia

(Received 4 April 2001; accepted for publication 16 May 2001)

Ultrafine-grained (UFG) Ti samples have been prepared using equal channel angular pressing followed by cold rolling and annealing. The deformation behavior of these materials, including strain hardening, strain rate dependence of flow stress, deformation/failure mode, and tensile necking instability, have been systematically characterized. The findings are compared with those for conventional coarse-grained Ti and used to explain the limited tensile ductility observed so far for UFG or nanocrystalline metals. © *2001 American Institute of Physics.*
[DOI: 10.1063/1.1384000]

Despite extensive research over the past decade, the deformation behavior of nanocrystalline (nc) and ultrafine-grained (UFG, grain sizes $<\sim 300$ nm) metals still remains poorly understood.[1–4] It is well established that the strength and hardness of nc and UFG metals are significantly enhanced over those of their coarse-grained (CG) counterparts, as expected from an extrapolation of the Hall–Petch relationship for CG materials. In contrast, the predicted retention and even increase of ductility,[5] extrapolated from experience with conventional materials, has rarely been observed. In fact, tensile elongation to failure observed for nc and UFG metals rarely exceeded 5%, even for metals that are very ductile at conventional grain sizes.[1,3] To understand such observations, it is useful to compare the tensile behavior with that in a compression test, as the latter is not as susceptible to minor processing flaws and avoids the problem of tensile necking instability. As such, compression test results can reveal the intrinsic behavior of the material and be used to predict/explain the tensile properties.[6] Unfortunately, there have been only a handful of published tensile and compressive stress–strain curves.[1–3] Particularly important is a systematic probing into the strain hardening as well as strain rate hardening behavior, as they determine the onset and propagation of plastic instabilities, such as necking or shear localization. Such information can often be obtained from compression tests even when a material exhibits very limited plastic deformation in tension. In addition, it is useful to document the deformation mode, such as shear banding or necking versus uniform deformation, under different loading conditions and at various stages of plastic deformation. The goal of this work on UFG Ti is to conduct a study covering all these aspects. The insight gained will shed light on the mechanical behavior of nc and UFG metals, in general.

The UFG-Ti was processed by equal channel angular pressing (ECAP) (eight passes) of commercial pure α titanium at 450 °C followed by cold rolling (CR) to a cross sectional area reduction of 73%. The details of the material microstructure and the processing procedures have been given elsewhere.[7–10] As-processed (ECAP+CR) grains were elongated along the longitudinal rolling direction and relatively more equiaxed in the transverse cross section, with an average grain size of $\sim$260 nm.[10] Some UFG-Ti samples were annealed at 300 °C for 30 min in Ar, to produce recovery of the dislocation structures and an associated decrease in internal stress, without causing grain growth.[7] CG-Ti was prepared by annealing a commercial Ti at 705 °C for 2 h and then air cooling, resulting in equiaxed grains averaging 35 μm in size. The quasistatic uniaxial tensile and compression tests were performed at strain rates of $1-4\times10^{-4}\,s^{-1}$. The high-strain-rate compression tests were performed using the Kolsky Bar technique[11] at strain rates of $2-9\times10^{+3}\,s^{-1}$. The compression tests used cylindrical samples from 2.7 to 3 mm in diameter. The specimen length was 4.5 mm for quasistatic tests, and 3.0 mm for high-rate tests.

Figure 1 shows a true stress–strain curve for the as-processed UFG-Ti in comparison with that for the CG-Ti, obtained under uniaxial compression at $2\times10^{-4}\,s^{-1}$. At a strain of 6%, the flow stress of the UFG-Ti (1.02 GPa) is more than twice that of CG-Ti (0.45 GPa), consistent with the known Hall–Petch relationship for conventional Ti.[12] The as-processed UFG-Ti exhibits little strain hardening, with a nearly perfectly plastic behavior at strains above 5%. In comparison, CG-Ti shows obvious strain hardening, part of which is due to deformation twinning.[13,14] Strain hardening appears to diminish with decreasing grain sizes[12] and is largely inhibited in the heavily cold worked UFG-Ti. The stress–strain curve for UFG-Ti after annealing is also included in Fig. 1. Compared with the as-processed case, the yield strength of the annealed UFG-Ti is lower. The strain-hardening rate, on the other hand, is higher than the as-processed case for strains less than $\sim$5%, which is attributable to the recovery of the cold-worked grains. However, due to the small grain sizes, the capacity for the accumulation of dislocations and twin boundaries and hence strain hardening remains very limited and far less than that of CG-Ti.

This difference in the strain hardening capacity between

a)Electronic mail: ema@jhu.edu

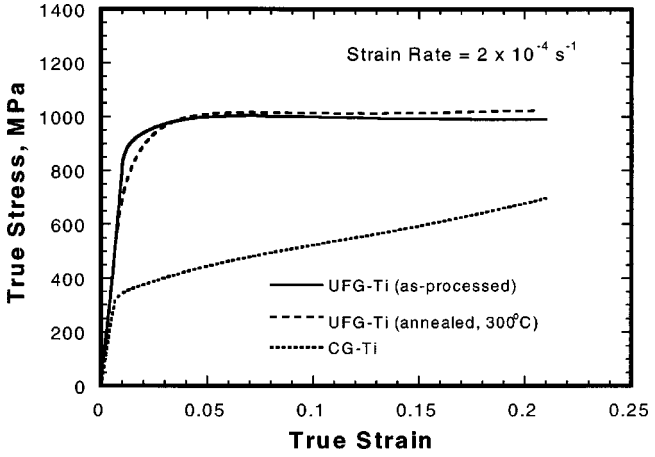

FIG. 1. Typical compressive true stress–strain curves for UFG-Ti (as-processed and annealed) at a quasistatic-strain rate, with a curve for CG-Ti for comparison are shown.

the UFG-Ti and CG-Ti, and between the as-processed and annealed UFG-Ti, is expected to affect the maximum uniform strain prior to necking under uniaxial tension. The well known Considere criterion for necking,

$$\left(\frac{\partial\sigma}{\partial\epsilon}\right)_{\dot{\epsilon}} = \sigma, \tag{1}$$

where σ and ϵ are true stress and true strain, respectively, predicts that the as-processed UFG-Ti, with little capacity for strain hardening, would become unstable soon after the onset of plastic strain. The annealed UFG-Ti, with some regained capacity for strain hardening, would be mechanically stable initially until the rate of work hardening falls to such a level that the condition of Eq. (1) is reached, which occurs at a strain of approximately ~5%. The higher strain hardening of the annealed UFG-Ti would also help overcome softening caused by flaws or damage sites operative in tension. These predictions agree well with the tension test curves [Fig. 2(a)] and the necking morphology [Fig. 2(b)] we observe. The tensile fracture surface also shows clear ductile (cup and cone) features [Fig. 2(c)], as expected from the large ductility seen in compression. In essence, the capacity for uniform straining has been "used up" in the as-processed UFG-Ti, and remains fairly small after annealing because even after recovery the small grains have limited room left for strain hardening mechanisms to operate. In comparison, CG-Ti exhibits much larger uniform deformation in tension before the necking condition is reached [see Eq. (1)]. In terms of the strain hardening exponent n, the shapes of the stress–strain curves in Fig. 2 do not yield a constant value. Eq. (1), rather than n, is therefore a more reliable method to estimate the amount of maximum tensile uniform deformation at the onset of necking. For comparison purposes, we estimated an average n of about 0.2 for the CG-Ti. It drops to 0.04 for the annealed UFG-Ti. These values are consistent with the maximum strains prior to necking seen in Fig. 2.

A typical true stress–strain curve for the annealed UFG-Ti at a high-strain rate of $3.4\times10^{+3}\,\mathrm{s}^{-1}$ is compared with a quasistatic curve in Fig. 3(a), together with two corresponding curves for the CG-Ti at similar strain rates. The strain-rate dependence of the flow stress at a constant strain of 6% is plotted in Fig. 3(b) for the strain-rate range from

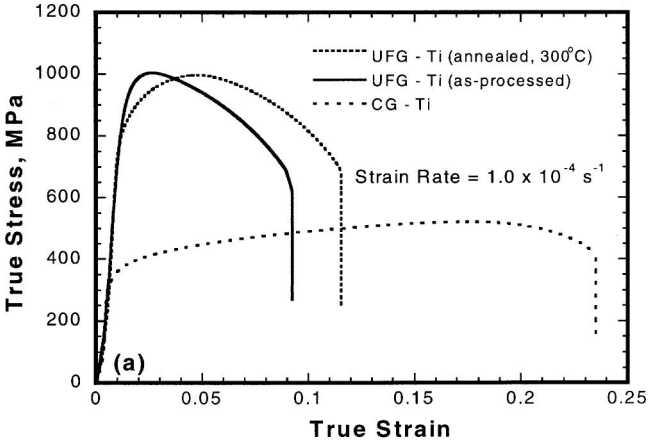

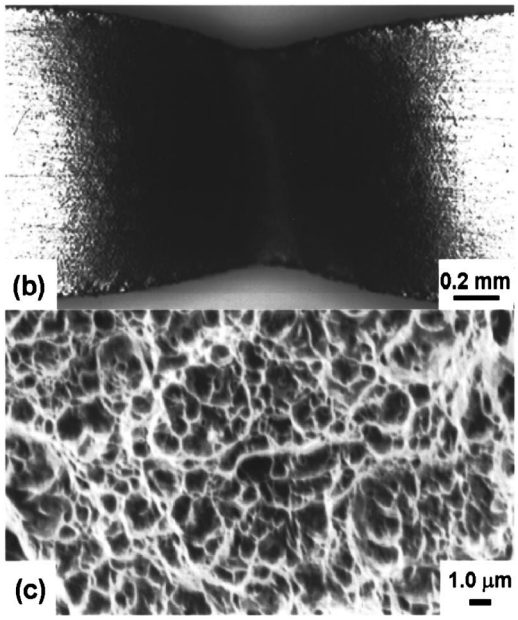

FIG. 2. (a) Tensile true stress–strain curves for as-processed and annealed UFG-Ti, in comparison with that of CG-Ti. (b) Optical micrograph showing necking in the annealed UFG-Ti, (c) scanning electron microscopy of typical ductile features on the fracture surface of the sample in (b).

2×10^{-4} to $9\times10^{+3}\,\mathrm{s}^{-1}$. If a linear relationship is assumed,[13] the UFG-Ti and CG-Ti lines have similar slopes, $(\partial\sigma/\partial\ln\dot{\epsilon})_{\epsilon}$, indicating that the magnitude of the strain-rate enhancement of the flow stress (~200 MPa) is similar for these two very different grain sizes. However, due to the elevated strength of UFG-Ti, the strain rate sensitivity, m, defined as $(\partial\ln\sigma/\partial\ln\dot{\epsilon})_{\epsilon}=(1/\sigma)(\partial\sigma/\partial\ln\dot{\epsilon})_{\epsilon}$, drops by a factor of 2–3 relative to that for CG-Ti (from 0.025 to 0.009).

Hart's instability criterion for rate-sensitive materials,[15]

$$\frac{1}{\sigma}\left(\frac{\partial\sigma}{\partial\epsilon}\right)_{\dot{\epsilon}} - 1 + m = 0, \tag{2}$$

indicates that the value of m affects the necking instability and therefore the ductility measured in a uniaxial tensile test (the material with a higher value of m is more stable). Thus, the low m renders the UFG-Ti less resistant to necking, and contributes to the fast post necking softening and reduced elongation to failure observed in Fig. 2.

In quasistatic compression tests, both the UFG-Ti and the CG-Ti exhibit only uniform deformation. No softening

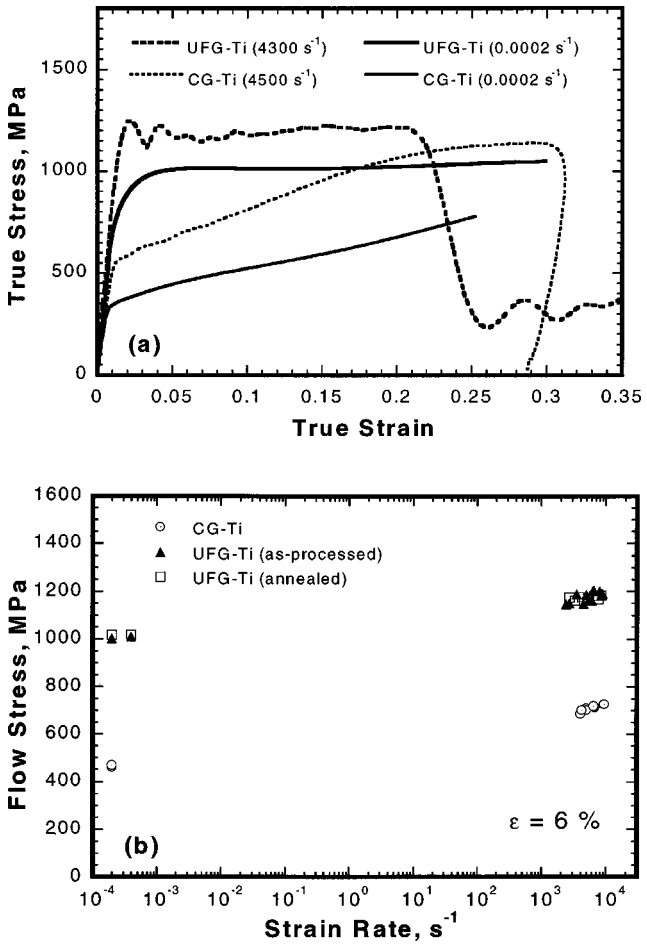

FIG. 3. (a) Comparison of high-strain-rate true stress–strain curves with those at quasistatic-strain rates for both the annealed UFG-Ti and CG-Ti are shown. Shear failure occurred at a strain of ~22% at a high rate for UFG-Ti, while all other curves ended with unloading. (b) Strain-rate dependence of the flow stress of UFG-Ti and CG-Ti at a strain of 6% is presented.

was observed in the stress–strain curves up to high strains where the tests were stopped by unloading. Therefore, the early softening observed in tension (Fig. 2) can be attributed entirely to the necking phenomenon, i.e., the geometric tensile "structural" instability. The comparison between UFG-Ti and CG-Ti illustrates the point that the necking instability is exacerbated in high strength UFG and nc metals, as predicted by Eqs. (1) and (2).

At the high-strain rates of $4-9\times10^{+3}\,s^{-1}$, on the other hand, apparent softening does occur under uniaxial compression in the UFG-Ti at strains of 20–24%, followed by a catastrophic failure. These failures, occurring only at high-strain rates, are believed to be the result of *adiabatic* shear banding.[16] Observation of the fracture surfaces, which are oriented along a diagonal direction of the specimen, supports the hypothesis that the failure was caused by adiabatic shearing. Note that such a failure mode did not occur in CG-Ti until a much higher true strain (~60%). The higher propensity of UFG-Ti for (adiabatic) shear banding than the CG-Ti can be explained on the basis of the observed low-strain hardening and low-rate sensitivity.[16] It has been shown[16,17] using simple constitutive laws that a reduced n (e.g., an increased strength and/or a reduced strain-hardening rate $\partial\sigma/\partial\epsilon$), and/or a reduced m, can lead to a reduced critical shear strain for adiabatic shear banding. The localization of the deformation into adiabatic shear bands thus commences earlier in our UFG-Ti. Another example of instability was seen in consolidated nc and UFG-Fe, where the shear banding mode dominates from the onset of plastic deformation even at quasistatic strain rates[18] (not necessarily due to adiabatic phenomena in this case).

In summary, mechanical responses of UFG-Ti in comparison with CG-Ti have been systematically characterized. Compression test results are found very useful in rationalizing the observed tensile behaviors. The high strength of a UFG metal is in accordance with the Hall–Petch relationship. The UFG-Ti is clearly ductile, in compression as well as during tensile fracture. However, such UFG metals, and nc metals as well due to the diminishing dislocation activities, tend to lose the defect accumulation mechanisms and hence the capacity for strain hardening.[1] Meanwhile, the strain rate sensitivity is also reduced. As a result, the tendency for plastic instabilities is enhanced. In tension, the necking instability sets in early. This is a structural, rather than intrinsic, softening response inherent to the tensile test geometry. This vulnerability to localized deformation/failure modes, in addition to sample flaws, is believed to be at least partly responsible for the limited tensile uniform deformation and elongation to failure observed so far for the vast majority of nc and UFG materials that are ductile at conventional grain sizes or in compression tests.[1,3] Also, (adiabatic) shear banding is promoted in lieu of uniform deformation, especially at high-strain rates. This enhanced tendency for shear localization, nevertheless, has potential value in applications such as kinetic energy penetrators.

The authors thank D. Olson and C.-H. Shang for experimental assistance. This work is supported by ARO-DAAD19-01-2-0003 and by NSF-CMS-9877006.

[1] C. C. Koch, J. Nanoscience Technol. (in press).
[2] J. R. Weertman, D. Farkas, K. Hemker, H. Kung, M. Mayo, R. Mitra, and H. Swygenhoven, MRS Bull. **24**, 44 (1999).
[3] C. C. Koch, D. G. Morris, K. Lu, and A. Inoue, MRS Bull. **24**, 54 (1999).
[4] P. G. Sanders, C. J. Youngdahl, and J. R. Weertman, Mater. Sci. Eng., A **234**, 77 (1997).
[5] R. Bohn, T. Houbold, R. Birringer, and H. Gleiter, Scr. Metall. Mater. **25**, 811 (1991).
[6] J. A. Eastman, M. Choudry, M. N. Rittner, C. J. Youngdahl, M. Dollar, J. R. Weertman, R. J. DiMelfi, and L. J. Thompson, in *Chemistry and Physics of Nanostructures and Related Nonequilibrium Materials*, edited by E. Ma, B. Fultz, R. Shull, J. Morral, and P. Nash (The Minerals, Metals, and Materials Society, Warrendale, PA, 1997).
[7] A. A. Popov, I. Y. Pyshmintsev, S. L. Demakov, A. G. Illariinov, T. C. Lowe, A. V. Sergeyeva, and R. Z. Valiev, Scr. Mater. **37**, 1089 (1997).
[8] V. V. Stolyarov, Y. T. Zhu, T. C. Lowe, and R. Z. Valiev, Mater. Sci. Eng., A **303**, 82 (2001).
[9] V. V. Stolyarov, Y. T. Zhu, I. V. Alexandrov, T. C. Lowe, and R. Z. Valiev, Mater. Sci. Eng., A **299**, 59 (2001).
[10] MRS Bull. **25**, 13 (2000).
[11] P. S. Follansbee, *Metal Handbook*, edited by J. R. Davis (American Society for Metals, Metals Park, Ohio, 1985), Vol. 8, p. 198.
[12] R. J. Jones and H. Conrad, Trans. Metall. Soc. AIME **245**, 779 (1968).
[13] D. R. Chichili, K. T. Ramesh, and K. J. Hemker, Acta Mater. **46**, 1025 (1998).
[14] S. Nemat-Nasser, W. G. Guo, and J. Y. Cheng, Acta Mater. **47**, 3705 (1999).
[15] E. W. Hart, Acta Mater. **15**, 351 (1967).
[16] Y. L. Bai and B. Dodd, *Adiabatic Shear Localization: Occurrence, Theories and Applications* (Pergamon, Oxford, 1992).
[17] M. R. Staker, Acta Metall. **29**, 683 (1981).
[18] D. Jia, K. T. Ramesh, and E. Ma, Scr. Mater. **42**, 73 (2000).